ADVANCED FUNCTIONAL MATERIALS
www.afm-journal.de

Materials Views
www.MaterialsViews.com

Charge-Compensated Compound Defects in Ga-containing Thermoelectric Skutterudites

Yuting Qiu, Lili Xi, Xun Shi, Pengfei Qiu, Wenqing Zhang,* Lidong Chen, James R. Salvador, Jung Y. Cho, Jihui Yang, Yuan-chun Chien, Sinn-wen Chen, Yinglu Tang, and G. Jeffrey Snyder**

Heavy doping changes an intrinsic semiconductor into a metallic conductor by the introduction of impurity states. However, Ga impurities in thermoelectric skutterudite $CoSb_3$ with lattice voids provides an example to the contrary. Because of dual-site occupancy of the single Ga impurity charge-compensated compound defects are formed. By combining first-principle calculations and experiments, we show that Ga atoms occupy both the void and Sb sites in $CoSb_3$ and couple with each other. The donated electrons from the void-filling Ga (Ga_{VF}) saturate the dangling bonds from the Sb-substitutional Ga (Ga_{Sb}). The stabilization of Ga impurity as a compound defect extends the region of skutterudite phase stability toward $Ga_{0.15}Co_4Sb_{11.95}$ whereas the solid–solution region in other directions of the ternary phase diagram is much smaller. A proposed ternary phase diagram for Ga-Co-Sb is given. This compensated defect complex leads to a nearly intrinsic semiconductor with heavy Ga doping in $CoSb_3$ and a much reduced lattice thermal conductivity (κ_L) which can also be attributed to the effective scattering of both the low- and high-frequency lattice phonons by the dual-site occupant Ga impurities. Such a system maintains a low carrier concentration and therefore high thermopower, and the thermoelectric figure of merit quickly increases to 0.7 at a Ga doping content as low as 0.1 per Co_4Sb_{12} and low carrier concentrations on the order of 10^{19} cm^{-3}.

1. Introduction

Doping in semiconductors introduces impurity defects into the system that could significantly change its electrical, thermal transport, or optical properties.[1–6] In thermoelectric materials, aliovalent defects are usually introduced to add or subtract electrons from the bands to tune the carrier concentration, which is essential to achieving optimal dopant concentrations and an optimized performance.[7–9] The addition of an impurity element usually forms one dominant type of defect, and the material will be turned into an n-type or p-type semiconductor. However, in wide-bandgap materials such as oxides, the energy required to add or subtract an electron from the conduction or valence band is so high that compensating defects are often formed.[10–13] Frenkel and Schottky defects, with charge-balanced complexes that contain different anions and cations, are common examples of compound defects that are formed to thermodynamically compensate for the effects of electronic doping.[14–16]

Skutterudite compounds, having an unusual caged structure, are excellent narrow-bandgap thermoelectric materials at intermediate temperatures.[1,4] Binary skutterudites have a general formula MX_3, where M is Co, Rh, or Ir, and X is a pnictogen such as P, As, or Sb. They crystallize into a body-centered-cubic structure (Im-3). A conventional unit cell contains 32 atoms arranged in

Dr. Y. Qiu, L. Xi, Prof. X. Shi, P. Qiu, W. Zhang, L. Chen
State Key Laboratory of High Performance Ceramics and Superfine Microstructure
Shanghai Institute of Ceramics
Chinese Academy of Sciences
Shanghai 200050, China
E-mail: xshi@mail.sic.ac.cn; wqzhang@mail.sic.ac.cn
Dr. J. R. Salvador, J. Y. Cho
Chemical and Materials Systems Lab
General Motors R&D Center
Warren, MI 48090, USA
Dr. Y. Qiu
University of Chinese Academy of Sciences
Beijing 100049, China
Prof. J. Yang
Materials Science & Engineering Department
University of Washington
Seattle, WA 98195, USA
Dr. Y.-c. Chien, Prof. S.-w. Chen
Department of Chemical Engineering
National Tsing Hua University
Hsin-Chu 300, Taiwan
Y. Tang, Dr. G. J. Snyder
Department of Materials Science
California Institute of Technology
Pasadena, CA 91125, USA
E-mail: jsnyder@caltech.edu

DOI: 10.1002/adfm.201202571

eight groups of MX_3 blocks. The transition metal M occupies the 8*c*-sites and the pnictogen atoms (*X*) occupy the 24*g*-sites to form MX_6 octahedra with the metal atom *M* in the center. There are two large lattice voids (icosahedral voids) at the 2*a* sites, which are surrounded by 12 *X* atoms.[3] Therefore, the chemical formula of skutterudite structures can also be written as VFM_4X_{12}, where VF represents the void-filling site. Impurities in thermoelectric skutterudites are typically described in terms of a single defect type. This is quite reasonable for many impurity atoms as the chemistry of each site in the structure dictates which defect type is likely to dominate.[17–19] Large alkali,[20–23] alkaline earth,[17,24,25] or lanthanoid metals[8,26–30] are too big for the transition metal site, but would fit into the large voids, donating their valence electrons to the $CoSb_3$ framework resulting in n-type materials.

The nature of group 13 impurities in $CoSb_3$, particularly Ga and In, has generated much debate because these Ga- or In-doped materials were found to show high thermoelectric figures of merit,[31–34] but the nature of this form of doping is still a matter of ongoing debate. At first it was assumed that group 13 elements occupy the void positions exclusively and donate electrons, which results in n-type ternary materials. Tl was expected to donate one electron in $CoSb_3$,[35–38] but for In and Ga it is not clear whether one or three electrons would be donated by void filling.[31–34,39–44] It was also predicted that such filling of group 13 elements is energetically unfavorable.[8] Several studies have shown GaSb- and InSb- containing composites were formed and it was concluded that Ga and In have virtually no solubility in $CoSb_3$.[39,41,43,45–47] There was yet another report claiming that In could possibly substitute Sb in $CoSb_3$ with little to no substitution on the void position.[33] Finally, as Ga^{3+} and In^{3+} are similar in size to Co^{3+}, it may also be possible for these atoms to substitute the transition metals.

Complicating this debate is the possibility that there is no dominant single defect type in skutterudites with group 13 elements, but that compound defects are formed similar to those found in wide-bandgap oxides. Amphoteric impurities were also observed in a few thermoelectric materials[48] in which a single impurity type formed both donor and acceptor defects. If both donor and acceptor defects exist, and form in equal amounts the material will be nearly fully compensated with few free carriers.[49]

In this study, we show both theoretical and experimental evidence for the presence of charge-compensated compound defects in $CoSb_3$ with Ga impurities. In this dual-site occupant system, $(Ga_{VF})_xCo_4Sb_{12-x/2}(Ga_{Sb})_{x/2}$, the presence of the Ga_{VF}-Ga_{Sb} compound defects naturally explains the transport data and sheds light on the debate concerning the occupancy of not only Ga but also In and Tl in skutterudites. Such amphoteric dopants are also expected to affect the filling behavior of alkaline-earth or rare earths in (Yb,Ga)- or (Ba,In)- dual filled $CoSb_3$ because current results suggest that group 13 elements may reduce the carrier concentration by substitutionally occupying the Sb sites.[47,50] Owing to the charge-compensated compound defects, $CoSb_3$ with Ga impurities shows intrinsic-semiconductor-like electrical transport properties with low carrier concentrations and very large thermopowers. Also, the dual-site occupancy induces a wide frequency range of lattice phonons through a combination of point-defect scattering from the Ga_{Sb} and resonant scattering from the filler, leading to a substantial reduction in lattice thermal conductivity (κ_L) and a rapid increase of the thermoelectric figure of merit zT in $CoSb_3$ with Ga impurities.

2. Results and Discussion

2.1. Structural Characterizations and Phase Diagram

2.1.1. Theoretical Identification of Stable Phases

Group 13 elements can be substituting at the void (2*a*), Sb (24*g*) and Co (8*c*) sites. The chemical reactions and the corresponding Gibbs free energies per Ga for these different substitutional scenarios can be written as follows:

$$4CoSb_3 + xGa \rightarrow (Ga_{VF})_xCo_4Sb_{12}$$
$$\Delta G_1 = (E_{(Ga_{VF})_xCo_4Sb_{12}} - T\Delta S + x\Delta F_v - 4\mu_{CoSb_3} - x\mu_{Ga})/x \quad (1)$$

$$4CoSb_3 + xGa \rightarrow Co_{4-x}(Ga_{Co})_xSb_{12} + xCo$$
$$\Delta G_2 = (E_{Co_{4-x}(Ga_{Co})_xSb_{12}} - T\Delta S + x\mu_{Co} - 4\mu_{CoSb_3} - x\mu_{Ga})/x \quad (2)$$

$$4CoSb_3 + xGa \rightarrow Co_4Sb_{12-x}(Ga_{Sb})_x + xSb$$
$$\Delta G_3 = (E_{Co_4Sb_{12-x}(Ga_{Sb})_x} - T\Delta S + x\mu_{Sb} - 4\mu_{CoSb_3} - x\mu_{Ga})/x \quad (3)$$

Here x is the fraction of filling or substitution. E_U is the calculated total energy of U ($U = (Ga_{VF})_xCo_4Sb_{12}$, $Co_{4-x}(Ga_{Co})_xSb_{12}$, $Co_4Sb_{12-x}(Ga_{Sb})_x$), μ_R is the chemical potential for the chemical species R, and ΔF_V is the vibration contribution to the Gibbs free energy per filler atom in the voids; ΔS is the configuration entropy due to the random distribution of fillers in $CoSb_3$. The doped Ga atoms are in the voids for Equation 1, at the Co sites for Equation 2, and at the Sb sites for Equation 3. The possibility of Ga substituting for Co can be easily excluded as the calculated Gibbs free energy of Equation 2 is always much higher than those of Equation 1 and 3.

The calculated Gibbs free energies (ΔG_1 and ΔG_3) from Equation 1 and 3 are shown in **Figure 1**a. They are positive over nearly the entire composition range, even though the entropy from the random distribution of the Ga atoms at the voids or Sb sites is taken into account at high temperatures. This indicates that Ga-related defects are thermodynamically unstable if the Ga atoms only fill the voids or only substitute Sb at the framework of $CoSb_3$ as a single defect type, implying Ga is not a dopant that has a large effect on the transport properties of skutterudites. However, this conclusion is in direct contradiction with the experimental reports that the transport properties are always altered in Ga-doped skutterudites, including reported n-type semiconducting behavior related to Ga atoms that were speculated to be in the voids. Pure binary $CoSb_3$ by contrast is usually a p-type semiconductor. We therefore consider some other Ga occupancy possibilities beyond the single defects, most likely a compound defect or defect complex must be present in Ga-containing skutterudites. Considering the low electron concentration and electrical conductivity observed for Ga-containing $CoSb_3$, a charge-compensating defect complex is expected. The most reasonable explanation is that Ga atoms may simultaneously occupy the void and Sb sites resulting in

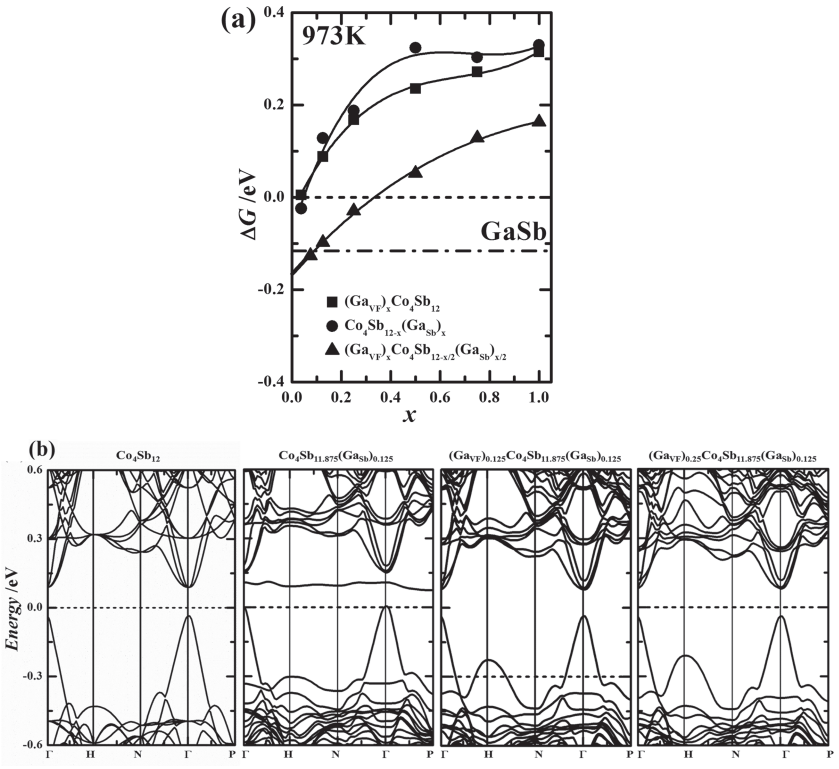

Figure 1. a) Calculated Gibbs free energy (ΔG) as a function of doping content of Ga in $CoSb_3$ skutterudite at 923 K. b) The calculated band structure of Co_4Sb_{12}, $Co_4Sb_{12-x}(Ga_{Sb})_x$, $(Ga_{VF})_xCo_4Sb_{12-x}(Ga_{Sb})_x$, and $(Ga_{VF})_xCo_4Sb_{12-x/2}(Ga_{Sb})_{x/2}$. The flat unoccupied band is related to a Ga-substitution-induced dangling bond and is clearly shown in the second picture of Figure 1b. A stable material with charge-compensated compound defects (the fourth picture of Figure 1b) has a band structure similar to binary $CoSb_3$ without dangling bonds.

charge-compensated behavior as Ga at the 2*a* site would donate electrons whereas the Ga at the Sb site accepts them.

For such dual-occupancy compound defects, the chemical reaction, and the corresponding Gibbs energy per Ga are written as follows:

$$\begin{aligned} &4CoSb_3 + (x+y)Ga \rightarrow (Ga_{VF})_xCo_4Sb_{12-y}(Ga_{Sb})_y + ySb \\ &\Delta G_4 = [(E_{Ga_{VF})_xCo_4Sb_{12-y}(Ga_{Sb})_y} - T\Delta S + x\Delta F_v) \\ &+y\mu_{Sb} - 4\mu_{CoSb_3} - (x+y)\mu_{Ga}]/(x+y) \end{aligned} \quad (4)$$

where x is the filling fraction, y is the substituting fraction, and $E_{(Ga_{VF})_xCo_4Sb_{12-y}(Ga_{Sb})_y}$ is the total energy of $(Ga_{VF})_xCo_4Sb_{12-y}(Ga_{Sb})_y$. Ga atoms simultaneously enter both the voids and Sb 24*g* sites to form a compound defect and act as an amphoteric impurity. The low carrier concentration observed in Ga-containing $CoSb_3$ requires the Ga-related amphoteric compound defects to be charge compensated. We expect an effective charge state of +1 for Ga in the voids (see the details below). Therefore, the chemical formula for the Ga-containing $CoSb_3$ with charge-compensated compound defects could be written as $(Ga_{VF})_xCo_4Sb_{12-x/2}(Ga_{Sb})_{x/2}$. Figure 1a also shows the calculated ΔG_4 for $(Ga_{VF})_xCo_4Sb_{12-x/2}(Ga_{Sb})_{x/2}$ at 923 K, which possesses the lowest values and becomes negative at about $x \leq 0.25$. The formation energy (–0.116 eV) of GaSb, a known secondary phase in Ga-containing $CoSb_3$, is also shown in Figure 1a, and it can be seen that it is lower than ΔG_4 for $x \geq 0.08$, indicating that $(Ga_{VF})_xCo_4Sb_{12-x/2}(Ga_{Sb})_{x/2}$ is the most stable phase when x is lower than 0.08. In other words, the maximum filling fraction for Ga in Co_4Sb_{12} should be around 0.08, and the total fraction of Ga atoms in a unit of Co_4Sb_{12} should be around 0.12 (= 1.5*x*) at 923 K.

The underlying mechanism for the unstable single-type defects is related to the modification of the chemical bonds and electronic structures. Binary $CoSb_3$ is a narrow-bandgap semiconductor with all bonds saturated and the electronic levels fully occupied to the top of the valence band. The substitution of an Sb atom by Ga in the framework leads to one unsaturated Ga_{Sb}-based dangling bond, because Ga has two valence electrons less than Sb. The Ga-related defect level is located just above the Fermi level and is unoccupied, which leaves the system containing Ga_{Sb} unstable. As the void is filled by Ga, the electrons donated from the void-filling Ga (Ga_{VF}) saturate the Ga_{Sb}-related dangling bond or the unoccupied empty level. This shifts the Ga-related level deep into the valence band with full electron occupation which lowers the energy of the whole system and makes the Ga-containing $CoSb_3$ stable. With this charge-compensated dual-site occupancy of Ga impurities, the Ga-containing $CoSb_3$ shows an intrinsic-semiconductor-like electronic structure. Interestingly, the band structure of $(Ga_{VF})_xCo_4Sb_{12-x/2}(Ga_{Sb})_{x/2}$ is essentially unchanged from that of $CoSb_3$ (see Figure 1b), particularly the bandgap and the primary band structure characteristics close to the edge of the conduction and valence bands are alike. The effective charge state of Ga in the voids of skutterudites is determined by the energetic disposition of the outer 4s and 4p electrons. If two 4s electrons and one 4p electron are completely transferred to the skutterudite framework, the charge state of Ga is +3. If only the 4p electron is transferred, it is +1. Whereas $(Ga_{VF})_xCo_4Sb_{12-x/2}(Ga_{Sb})_{x/2}$ shows a semiconductor-like band structure (see Figure 1b), the Fermi level E_F in $(Ga_{VF})_xCo_4Sb_{12-x}(Ga_{Sb})_x$ with equal Ga atoms in the voids and Sb sites, is observed to be located deep in the valence band, leaving some band-edge states unoccupied. Therefore, the actual charge state of Ga_{VF} should be around +1. Two Ga ions at the void sites and one at the Sb-substitutional site form a fully charge-compensated compound defect complex, and the final E_F is located in the middle of the bandgap as shown in Figure 1b. The calculated Gibbs free energies shown in Figure 1a also indicate that the composition $(Ga_{VF})_xCo_4Sb_{12-x/2}(Ga_{Sb})_{x/2}$ is thermodynamically stable. Ga-containing $CoSb_3$ compounds with these compositions should thus be electronically similar to binary $CoSb_3$ semiconductors.

2.1.2. Structural Characterizations in Experiment and Phase Diagram

Powder XRD patterns for these Ga-containing samples (see Section 2.1.1) are shown in **Figure 2**a. All major reflections are

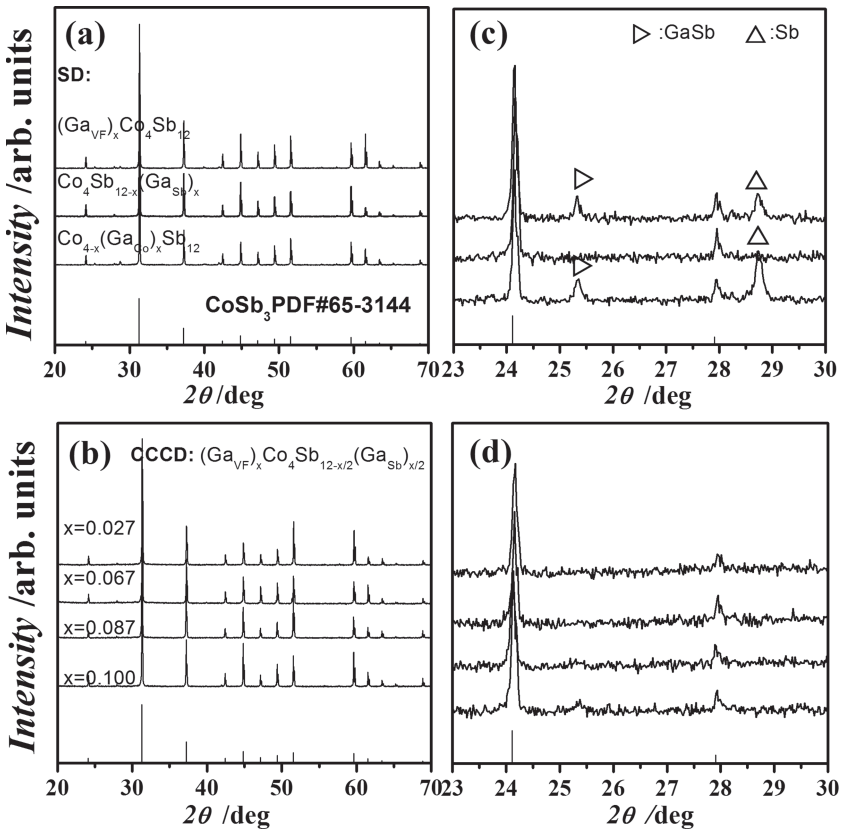

Figure 2. Powder XRD patterns of Ga-containing skutterudites with nominal compositions designed to realize a) the various single-type defects (SDs) and b) the charge-compensated compound defects (CCCDs). For SD samples, only the results for compounds where $x = 0.1$ are shown. For CCCD samples, the actual x values are estimated by EPMA analysis and indicated. c,d) Magnification of the powder XRD patterns of the polycrystalline SD (c) and CCCD (d) samples.

indexible to the skutterudite phase for samples with nominal composition $(Ga_{VF})_xCo_4Sb_{12-x/2}(Ga_{Sb})_{x/2}$, with no significant traces of impurities. However, small amounts of impurity phases, such as GaSb or Sb, are observed (see Figure 2b) in samples with nominal compositions designated as single-type defects, that is for $(Ga_{VF})_xCo_4Sb_{12}$, $Co_{4-x}(Ga_{Co})_xSb_{12}$, and $Co_4Sb_{12-x}(Ga_{Sb})_x$. The XRD data are consistent with our first-principles calculations shown in Section 2.1.1, indicating that the Ga impurity atoms are stabilized by the simultaneous occupancy of both the void and Sb sites.

Electron probe microanalysis (EPMA) measurements were carried out at four different locations on the samples, and the average compositions are listed in **Table 1**. The secondary X-ray maps show that there are many Ga-rich impurity phases in the single-type defect (SD) samples $(Ga_{VF})_xCo_4Sb_{12}$, $Co_{4-x}(Ga_{Co})_xSb_{12}$, and $Co_4Sb_{12-x}(Ga_{Sb})_x$. However, the Ga is nearly completely homogeneously distributed in the charge-compensated compound defect (CCCD) samples $(Ga_{VF})_xCo_4Sb_{12-x/2}(Ga_{Sb})_{x/2}$ (see **Figure 3**d). Furthermore, the Ga content in the single-type defect samples is very low even though high nominal Ga compositions were used for sample preparation. However, we could detect a relatively large Ga content close to the nominal compositions in the charge-compensated compound defect samples $(Ga_{VF})_xCo_4Sb_{12-x/2}(Ga_{Sb})_{x/2}$ (see 1) with few secondary phases. The total doping content and the maximum filling fraction in the voids for Ga in the charge-compensated compound defect samples are estimated to be around 0.15 and 0.1, respectively, according to EPMA data. This is consistent with our X-ray data and theoretical calculations, strongly supporting the proposition that impurity Ga atoms form charge-compensated compound defects in $CoSb_3$ by occupying both the void and Sb sites.

Table 1. Nominal Ga compositions, the total Ga compositions in the skutterudite phase estimated by EPMA, Seebeck coefficients (S), electrical conductivities (σ), and lattice thermal conductivities (κ_L) at 300 K for Ga-containing skutterudites with single-type defect and charge-compensated compound defect.

Samples	Nominal Ga Composition	Total Ga Composition	S [μV K^{-1}]	σ [×10^4 S m^{-1}]	κ_L [W m^{-1} K^{-1}]
$(Ga_{VF})_{0.1}Co_4Sb_{12}$	0.1	0.003	– 259.4	3.24	3.09
$(Ga_{VF})_{0.15}Co_4Sb_{12}$	0.15	0.020	– 351.5	1.35	5.06
$Co_{3.9}(Ga_{Co})_{0.1}Sb_{12}$	0.1	0.000	– 300.8	2.15	4.25
$Co_4Sb_{11.9}(Ga_{Sb})_{0.1}$	0.1	0.070	– 236.0	2.41	2.76
$Co_4Sb_{11.85}(Ga_{Sb})_{0.15}$	0.15	0.060	– 263.7	1.64	2.71
$(Ga_{VF})_{0.03}Co_4Sb_{11.985}(Ga_{Sb})_{0.015}$	0.045	0.040	– 286.6	1.11	3.47
$(Ga_{VF})_{0.06}Co_4Sb_{11.97}(Ga_{Sb})_{0.03}$	0.09	0.100	– 272.6	2.37	3.30
$(Ga_{VF})_{0.10}Co_4Sb_{11.95}(Ga_{Sb})_{0.05}$	0.15	0.130	– 228.6	4.44	3.15
$(Ga_{VF})_{0.15}Co_4Sb_{11.925}(Ga_{Sb})_{0.075}$	0.225	0.150	– 246.4	3.10	2.97

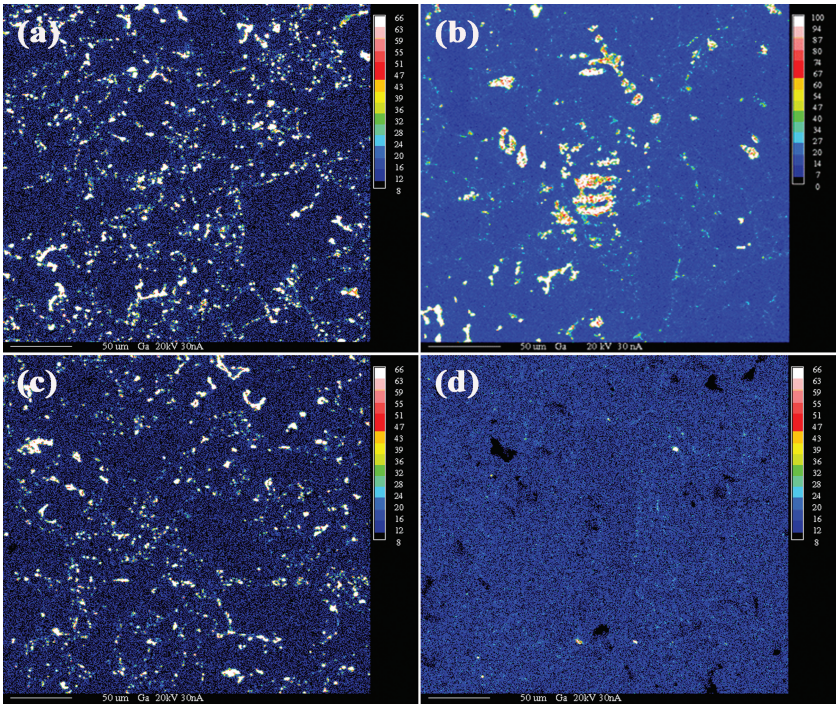

Figure 3. Secondary X-ray Ga maps in samples with different nominal compositions. a–c) Single-type defect (SD) samples $(Ga_{VF})_{0.10}Co_4Sb_{12}$ (a), $Co_4Sb_{11.9}(Ga_{Sb})_{0.10}$ (b), and $Co_{3.9}(Ga_{Co})_{0.10}Sb_{12}$ (c), and d) charge-compensated compound defect (CCCD) sample $(Ga_{VF})_{0.10}Co_4Sb_{11.95}(Ga_{Sb})_{0.05}$. The estimated compositions by EPMA are shown in Table 1.

phase. This was confirmed by the EPMA measurements; the results of which are listed in Table 1.

In the single-type defect samples a low Ga composition is always observed in the skutterudite phase areas, which is significantly less than the nominal composition and even less than the maximum Ga solubility ($x = 0.1$) along the $(Ga_{VF})_xCo_4Sb_{12-x/2}(Ga_{Sb})_{x/2}$ phase line. This can be explained by the equilibrium phase diagram we have constructed. The tie lines between the nominal composition and the equilibrium phase compositions are directed toward compositions with high Ga content in the impurity phases and low Ga content in the skutterudite phase. This is apparently the case on both sides of the stable $(Ga_{VF})_xCo_4Sb_{12-x/2}(Ga_{Sb})_{x/2}$ (red line) region, where nominal compositions slightly off this line produce a majority skutterudite phase, but with much less Ga than in the nominal composition. This may explain why a much lower solubility of Ga (and possibly In)[47] is often reported.[31] The higher Ga solubility in charge-compensated compound defect samples with dual defect composition $(Ga_{VF})_xCo_4Sb_{12-x/2}(Ga_{Sb})_{x/2}$ can be explained by the lower energy of the valence compensating defects calculated above.

The proposed phase diagram of the Ga-containing skutterudites at 923 K is shown in **Figure 4**a, and is based on general knowledge of binary phase diagrams.[51–55] The related binary phases of Ga, Co, and Sb are shown on the axes including the known regions of solid or liquid solubility for the binary compounds and a rough estimate of the solubility of the ternary compounds (red regions). The exact regions of solid solubility of GaSb, $CoSb_2$, and $CoSb_3$ are not known but they are enlarged for clarity in Figure 4a. The white regions of Figure 4a designate regions which are expected to contain two or three phases in equilibrium at 923 K.

The region near $CoSb_3$ is enlarged in Figure 4b. Our experimental data suggest that the region of Ga solubility is extended toward the charge-compensated compound defect samples, $(Ga_{VF})_xCo_4Sb_{12-x/2}(Ga_{Sb})_{x/2}$, with an estimated maximum x value around 0.1. Therefore, the nominal and experimental compositions of the charge-compensated compound defect samples with x values below 0.1 are situated on the red line shown in Figure 4b. When x exceeds 0.1, the charge-compensated compound defect samples contain a Ga-dual-position-doped skutterudite phase $(Ga_{VF})_{0.1}Co_4Sb_{11.95}(Ga_{Sb})_{0.05}$ and impurity phases GaSb and CoGa are expected. All single-type defect samples contain impurity phases regardless of the nominal Ga compositions used, which suggests the region of stability (red line) is narrow in directions other than along the $(Ga_{VF})_xCo_4Sb_{12-x/2}(Ga_{Sb})_{x/2}$ line. For example, samples with a nominal composition $Co_{4-x}(Ga_{Co})_xSb_{12}$ (triangles in Figure 4b) result in a $CoSb_3$-GaSb mixture with nearly no Ga incorporated into the skutterudite

2.2. Thermoelectric Properties

2.2.1. Electrical Transport

The Ga-containing charge-compensated compound defect skutterudites $(Ga_{VF})_xCo_4Sb_{12-x/2}(Ga_{Sb})_{x/2}$ exhibit transport properties different from other doped skutterudites. The temperature dependence of the thermoelectric transport properties are shown in **Figure 5**. Compared to alkali-metal-filled, alkaline-earth-filled, and rare-earth-filled $CoSb_3$, Ga-containing charge-compensated compound defect samples have a much lower electrical conductivity and much higher thermopower even when the actual Ga filling fraction is as high as 0.1 (see below for details). By assuming an effective charge state of +1 for Ga, as discussed above, Co_4Sb_{12} with 0.1 Ga in the voids should be nearly comparable with $Na_{0.13}Co_4Sb_{12}$. Our earlier work[23] showed that the room-temperature electrical conductivity and absolute thermopower in $Na_{0.13}Co_4Sb_{12}$ are around 0.9×10^5 S m^{-1} and 199 μV K^{-1}, respectively. However, the charge-compensated compound defect sample with a filling fraction of 0.1 Ga shows an electrical conductivity of only around (3-4) $\times 10^4$ S m^{-1}, which is much less than that of the Na-filled $CoSb_3$.[23] The absolute thermopower is about 250 μV K^{-1}.[23] Similar discrepancies have also been found between measured transport data for Ga-containing and Ba-filled $CoSb_3$.[24] Skutterudites with nominal single-type Ga defects, as shown in Figure 5, also show a low electrical conductivity but much higher thermopower. Based on the phase diagram (Figure 4) nominal single-type Ga doping

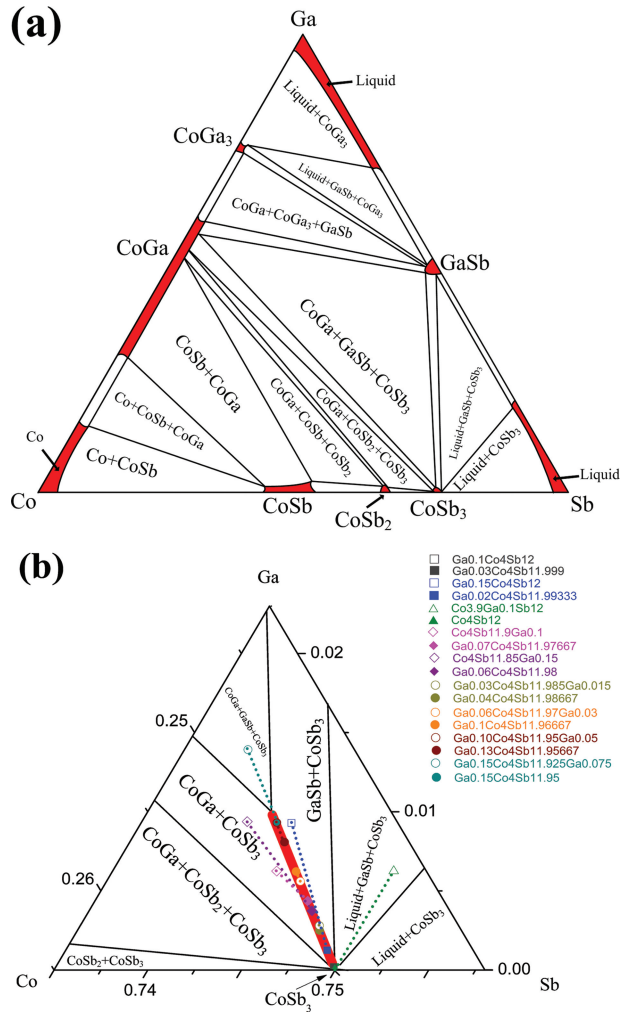

Figure 4. Proposed phase diagram for Ga-containing skutterudites at 923 K. a)Full diagram with related binary phases and approximate regions of solubility are shown in red and labeled on the axes. The regions of solubility for GaSb, $CoSb_2$ and $CoSb_3$ are enlarged for clarity. b)Region enlarged near $CoSb_3$. Because of the stability of Ga in dual-defect sites (charge-compensated compound defect samples) the region of Ga solubility is extended as a red line in the direction of $(Ga_{VF})_xCo_4Sb_{12-x/2}(Ga_{Sb})_{x/2}$ up to $x = 0.1$. The nominal sample compositions are shown as open symbols. Closed symbols represent the skutterudite composition ($(Ga_{VF})_xCo_4Sb_{12-x/2}(Ga_{Sb})_{x/2}$) of the major phase using the experimental EMPA value for Ga content, and are connected to the corresponding nominal sample composition with a dotted line. The expected regions of two and three equilibrium phases (white) have been adjusted to fit the experimental observations.

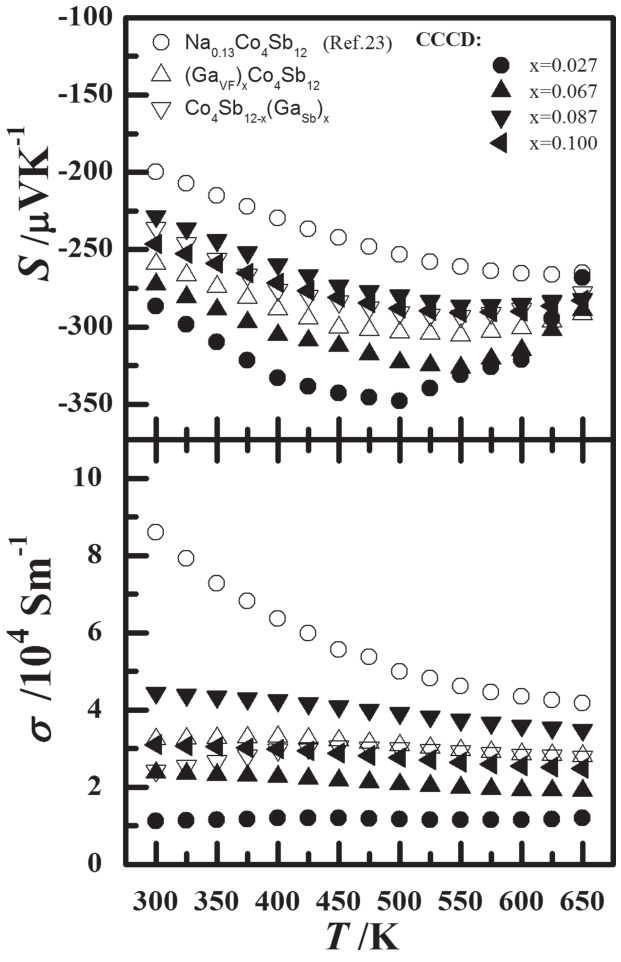

Figure 5. Temperature dependence of thermopower (S) and electrical conductivity (σ) for skutterudites with Ga-containing charge-compensated compound defects (CCCD). The electrical transport in Na-filled skutterudites and in samples with nominal compositions of $(Ga_{VF})_xCo_4Sb_{12}$ and $Co_4Sb_{12-x}(Ga_{Sb})_x$ ($x = 0.1$) are also shown for comparison.

in skutterudites results in charged-compensated Ga-containing skutterudites and impurity phases. Therefore, the samples with nominal compositions of single-type defects should be similar to those with charge-compensated defects, which is consistent with the data shown in Figure 5.

$CoSb_3$ is a valence precise semiconductor. Because Ga has two electrons less than Sb and Ga_{VF} has an effective charge state of +1, $(Ga_{VF})_xCo_4Sb_{12-x/2}(Ga_{Sb})_{x/2}$ should also be a valence precise semiconductor. Increasing the Ga doping content should not significantly change the carrier concentration if the actual composition does not deviate substantially from the ideal stoichiometry of the charge-compensated compound defect composition. This is further confirmed by the Hall data from present and previous measurements, in which very low carrier concentrations on the order of 10^{19} cm^{-3} were observed in group 13 containing skutterudites (see **Figure 6**) even with relatively high Ga doping content. Interestingly, the electron concentrations and their dependence on the Ga filling fraction x in the Ga-containing charge-compensated compound defect $CoSb_3$ follow the extended general trend of the $q \times x$ dependence of carrier concentrations from the alkaline metal- (AM-), alkaline earth- (AE-), and rare earth- (RE-) filled $CoSb_3$ although the values are shifted a little below the general trend line. The underlying mechanism is probably related to the low Ga incorporation in many experimental compositions (discussed above) and the net valence balance that the Ga charge-compensated compound defect imparts as compared to the normal filled-$CoSb_3$. It is certainly clear, however, that the measured electron concentrations, if referring to the as-reported nominal compositions for Ga-containing single-type defect $CoSb_3$ from the literature,[31]

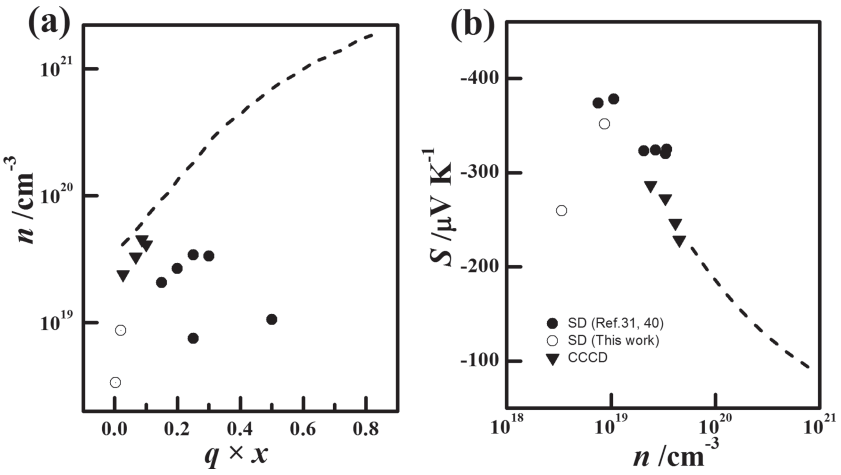

Figure 6. a) Room-temperature electron concentration (n) as a function of ($q \times x$) in Ga-containing charge-compensated compound defect (CCCD) skutterudites, where q is the filler effective charge state and x is the filling fraction. b) Room-temperature S as a function of electron concentration for Ga-containing CCCD skutterudites at 300 K. The x values were estimated by EPMA for our single-type defect and CCCD samples whereas they are the nominal values for the single-type defect samples from the literature.[31,40] The dashed lines represent the general trend of carrier concentration and thermopower for single filled-$CoSb_3$ with typical electropositive filler species taken from the literature.[17,22–24,26–30,32,56]

greatly deviate from the general trend as shown in Figure 6a. This is inconsistent with the assumption that Ga only enters the voids of $CoSb_3$ to form a single type of defect.

Consistent with the Ga-containing charge-compensated compound defect $(Ga_{VF})_xCo_4Sb_{12-x/2}(Ga_{Sb})_{x/2}$ being nearly an intrinsic semiconductor, all the $(Ga_{VF})_xCo_4Sb_{12-x/2}(Ga_{Sb})_{x/2}$ samples show relatively lower carrier concentrations as well as much higher thermopowers compared to Group 1, 2, or RE-filled $CoSb_3$.[30] As shown in Figure 6 the absolute thermopowers of the $(Ga_{VF})_xCo_4Sb_{12-x/2}(Ga_{Sb})_{x/2}$ compounds are still higher than 250 μV K^{-1} with electron concentrations less than 5×10^{19} cm^{-3} at room temperature (300 K). The S-n dependence in Ga-containing charge-compensated compound defect samples (and those in the literature[31,40]) follows the extrapolated curve of normal filled skutterudites. Figure 6 further indicates that the actual Ga composition in the single-type defect samples is very low (as observed in EMPA), leading to very low electron concentrations and large thermopowers. All data also provide strong evidence that the band structure in Ga-containing skutterudites are virtually unchanged near the Fermi level because the same trend is observed in the normally filled as well as in the Ga-containing skutterudites shown in Figure 6b. This is fully consistent with our band structure calculations shown in Figure 1b and discussions in Section 2.1.

2.2.2. Thermal Transport

All Ga-containing samples show a reduced κ_L as compared to binary $CoSb_3$ with κ_L values of around 10 W m^{-1} K^{-1} at 300 K.[1] However, compared to the observed κ_L reduction trends, especially the dependence of κ_L on the impurities filling fraction in the normal alkaline-earth- or rare-earth-filled $CoSb_3$, κ_L reduction in the Ga-containing charge-compensated compound defect samples have a much stronger dependence on the impurity content as shown in **Figure 7**c. Even at filling fractions lower than 0.10 κ_L was reduced to 3.5 W m^{-1} K^{-1} or less, which is lower than that measured for $Na_{0.13}Co_4Sb_{12}$.[23] The Ga-containing skutterudites with the nominal single-type defects also show a low total thermal conductivity and κ_L comparable to CCCD materials because of the same underlying mechanism as discussed in Section 2.2.1. As usual, κ_L is obtained by subtracting the electronic contribution from the total thermal conductivity (κ) using the Wiedemann–Franz law. Our first-principles calculations show that the Lorentz number for the charge-compensated Ga-containing skutterudites is 1.75×10^{-8} V^2 K^{-2} at 300 K, 2.0×10^{-8} V^2 K^{-2} at 650 K, and a little higher even at more elevated temperatures. We adopted an averaged value of 2.0×10^{-8} V^2 K^{-2} to simplify the estimation of the electronic thermal conductivity. The number is also consistent with the experimentally estimated value in our previous work [30] and is appropriate given the relatively low carrier concentration (ca. 10^{19} cm^{-3}) found in these samples.

The dramatic reduction of the lattice thermal conductivity in the charge-compensated compound defect samples could be explained by the dual-site occupation of Ga impurities and therefore a dual-character phonon scattering mechanism. The Ga impurity at the Sb-substitutional site is one type of typical point defect with size and mass mismatch compared to the host atoms, leading to the scattering of lattice phonons with relatively high frequencies. The Ga atoms at the void sites behave as a typical filler species and scatter long wavelength phonons via resonant scattering mechanisms. Indeed the filled Ga in $CoSb_3$ has a rattling or localized vibration frequency as low as 23 cm^{-1}, the lowest among all possible filler species.[29] Such low-frequency rattling could lead to very effective thermal conductivity reduction.[31] The above discussions and the effective κ_L reduction indicate that a broader spectrum of lattice phonons could be directly scattered in the Ga-containing charge-compensated compound defect skutterudites. The relatively high Ga doping concentration, when counting Ga impurities at both the void and Sb sites, could also play a role.

2.2.3. Thermoelectric Figures of Merit

For good thermoelectric materials with very low κ_L, zT ($zT = S^2\sigma T/\kappa$) is mainly determined by the thermopower S. As a special case of filled skutterudites, the CCCD $(Ga_{VF})_xCo_4Sb_{12-x/2}(Ga_{Sb})_{x/2}$ systems have a very low κ_L value while maintaining a very large S, leading to a significantly improved zT at relatively low filling fractions (see **Figure 8**). Furthermore, the maximum zT in $(Ga_{VF})_xCo_4Sb_{12-x/2}(Ga_{Sb})_{x/2}$ samples is quickly improved from around 0.3 to 0.7 at 600 K, when increasing the Ga filling fraction from 0.027 to 0.087 (see Figure 8), with a much stronger compositional dependence than that found for normal alkali-metal filled skutterudites. The underlying reason for this stronger dependence is the dual-character phonon

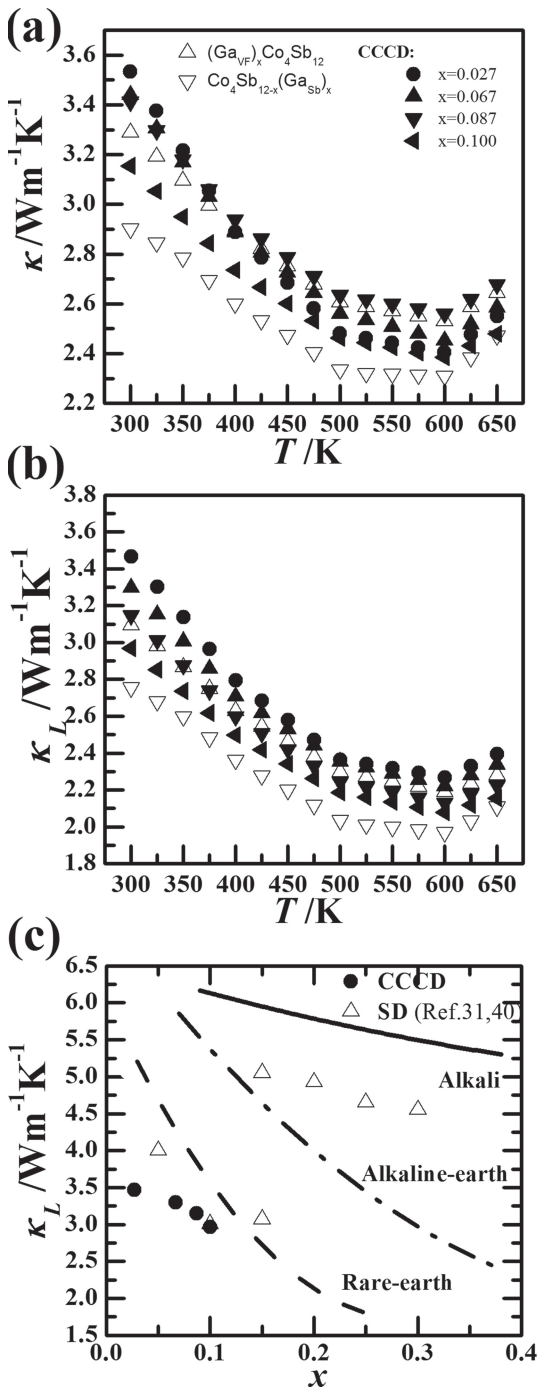

Figure 7. Temperature dependence of a) total thermal conductivity and b) lattice thermal conductivity (κ_L) for Ga-containing CCCD skutterudites. The κ and κ_L for samples with nominal compositions of $(Ga_{VF})_xCo_4Sb_{12}$ and $Co_4Sb_{12-x}(Ga_{Sb})_x$ ($x = 0.1$) are also shown for comparison. c) Room-temperature lattice thermal conductivity as a function of the filling fraction of impurities in skutterudites. The κ_L trends for alkaline- (solid line), alkaline-earth- (dashed-dotted line), and rare-earth- (dashed line) fillings are shown for comparison. The black dots represent the Ga-containing charge-compensated compound defect skutterudites in the present work, and the triangles represent the group 13 elements-doped single-type defect skutterudites reported previously[31,40] using the as-reported compositions.

scattering of the Ga-induced charge-compensated compound defects. A maximum zT value of 0.7 (at 600 K) is obtained in Ga-containing charge-compensated compound defect skutterudites with a Ga filling fraction $x = 0.087$ (Figure 8). All these indicate that the charge-compensated dual-site occupancy of single impurity-doped skutterudites can be used to design the compound defects, which are beneficial for the realization of high zT.

2.2.4. Discussion of Group 13 Elements in Double and Multiple Filled-Skutterudites

The detailed study on Ga impurities in $CoSb_3$ systems presented here may also shed light on the debate regarding other group 13 element doping in this system, particularly that of indium. Most likely other group 13 elements, especially In, have a similar tendency to form charge-compensated compound defects in $CoSb_3$. Recent work has demonstrated that group 13 elements-related double-filled or even multiple-filled skutterudites show excellent thermoelectric properties with some unusual phenomena.[33,39,41,43] For example, in In-Ba double-filled skutterudites,[50] the calculated electron concentration decreased when small amounts of In were introduced as an impurity. In In-Ce double-filled or multiple-filled skutterudites,[47] excess Sb and InSb phases were always observed together with the as-reported multiple dopants filled into the voids. Our previous work[43] has demonstrated that Ga-Yb double filling could be artificially manipulated to produce homogeneously distributed GaSb nanoparticles. All these examples imply that the interaction between group 13 elements as dual-character dopants and other usual fillers in $CoSb_3$ is quite complicated, and thus this is worth further investigations in the future.

3. Conclusions

We have demonstrated the amphoteric doping nature of Ga impurities and have shown that Ga impurities have a charge-compensated dual-site occupancy character with the ability to occupy both the 2*a* void-filling and Sb-24*g* sites. By combining first-principles calculations and experimental investigations, we have proven that the most stable formulations of Ga-containing skutterudites should be of the type $(Ga_{VF})_xCo_4Sb_{12-x/2}(Ga_{Sb})_{x/2}$ with charge-compensated compound defects. The Ga-containing charge-compensated compound defect $(Ga_{VF})_xCo_4Sb_{12-x/2}(Ga_{Sb})_{x/2}$ shows nearly intrinsic semiconducting behavior with a band structure that is similar to that of binary $CoSb_3$. For compositions close to $(Ga_{VF})_xCo_4Sb_{12-x/2}(Ga_{Sb})_{x/2}$, Ga-containing $CoSb_3$ demonstrated a low carrier concentration and large thermopower. Concommitantly the dual-site occupancy of a single Ga impurity leads to effective scattering of a wide range of lattice phonons and an unusually strong reduction in the lattice thermal conductivity with increasing Ga content resulting in a sharp increase of the thermoelectric figure of merit at low Ga doping. Our work points to a new approach for optimizing the performance of thermoelectric materials. We think by searching for impurities with charge-compensated dual-site occupancy character the κ_L can be decreased continually while maintaining a large *S*.

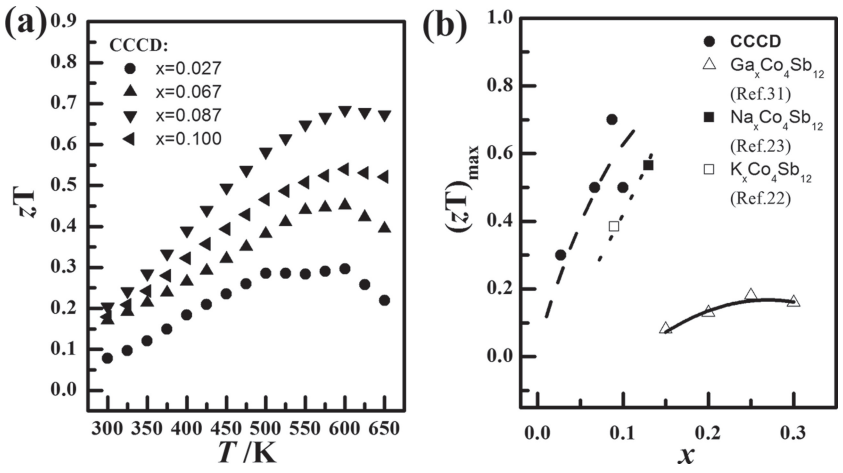

Figure 8. a) Temperature dependence of thermoelectric figure of merit (zT) for Ga-containing charge-compensated compound defect (CCCD) skutterudites. b) Maximum zT as a function of filling fraction x. The black line stands for $Ga_xCo_4Sb_{12}$ and is taken from a previous report.[31] The zT values of the Na- and K- filled skutterudites are also taken from the literature.[22,23]

4. Experimental Section

4.1. Sample Synthesis

As indicated above skutterudites have three different atomic positions: Co sites (8*c*), Sb sites (24*g*), and void sites (2*a*). We investigated four hypothetical cases corresponding to Ga occupancy exclusively at the 2*a* site, at the 8*c* site, at the 24*g* site; and a co-occupancy of Ga at both the 2*a* and 24*g* sites. To investigate these possibilities samples with nominal compositions $(Ga_{VF})_xCo_4Sb_{12}$, $Co_{4-x}(Ga_{Co})_xSb_{12}$, $Co_4Sb_{12-x}(Ga_{Sb})_x$, and $(Ga_{VF})_xCo_4Sb_{12-x/2}(Ga_{Sb})_{x/2}$ with x changing from 0.03 to 0.06, 0.10, and 0.15 were prepared by a combination process of melting and long-term high-temperature annealing. High-purity elements Co (99.99%, shot), Sb (99.9999%, piece), and Ga (99.999%, shot) were used as raw materials. Binary GaSb was prepared first, and then this was mixed with Co and Sb in their desired stoichiometric ratios. The mixture was placed in a boron nitride crucible, and then sealed in a fused silica tube under protecting Ar gas. The silica tubes and charges were heated slowly up to 1353 K, quenched to room temperature, followed by annealing at 923 K for one week. The resulting products were ground into fine powders, and consolidated by Spark Plasma Sintering (SPS) at 873 K under a pressure of 60 MPa, yielding fully dense bulk samples. A high-density (> 96% of the theoretical density) was achieved in all samples.

4.2. Structural Characterization

Room-temperature powder X-ray diffraction (XRD) data were collected on a D/max 2550V diffractometer using Cu Kα radiation to check phase purity and identity. Quantitative elemental analyses of the sintered samples were performed with a Cameca SX100 electron probe microanalysis (EPMA) using an accelerating voltage of 20 KeV and averaged over 4 randomly selected locations.

4.3. Thermoelectric Transport Properties

Electrical transport properties, including the electrical conductivity (σ) and Seebeck coefficient (S) were measured using a ZEM-3 (ULVAC Co. Ltd.) apparatus under a helium atmosphere in the temperature range of 300 to 650 K. The thermal conductivity (κ) was calculated using the measured thermal diffusivity, specific heat, and sample density. The thermal diffusivity and specific heat were measured in an argon atmosphere using the laser flash method (NETZSCH LFA 427) and differential scanning calorimetry (NETZSCH 404F3), respectively. The density of the samples was measured using the Archimedes method. Hall coefficients (R_H) were measured using a quantum-design physical property measurement system (PPMS) by sweeping the magnetic field up to 3T in both positive and negative directions. The Hall carrier concentration (n) was then estimated to be equal to $1/R_He$, where e is the elementary charge. The Hall carrier mobility (μ_n) was calculated according to the relation $\mu_n = R_H\,\sigma$. The estimated measurement accuracies are listed below for the commercial equipment used: 5% for electrical resistivity, 7% for thermopower, 5% for thermal diffusivity and 1% for density. Thus the combined uncertainty for ZT was about 20%.

4.4. First-Principles Calculations

All calculations were carried out using the projector augmented wave (PAW) method, as implemented in the Vienna *ab initio* Simulation Package (VASP),[57,58] and the Perdew-Burke-Ernzerhof generalized gradient approximation (GGA) for the exchange-correlation potential was used for all the calculations. Please refer to our earlier publications for computational details.[8,29,43] All calculations of pure and doped $CoSb_3$ skutterudites were carried out using a supercell ($2 \times 2 \times 2$ primitive cell) with a total of 128 atoms and 8 voids. A $3 \times 3 \times 3$ Monkhorst-Pack uniform k-point sampling was used for total energy calculations of the supercell and $15 \times 15 \times 15$ Monkhorst-Pack uniform k-point sampling was used for other compounds. Lattice constants and ion positions were optimized. Different configuration structures were considered and the ones with the lowest total energy were used for further analysis. The Lorentz number calculations were carried out within the framework discussed in the literature.[59]

Supporting Information

Supporting Information is available from the Wiley Online Library or from the author.

Acknowledgements

This work was supported by the National Basic Research Program of China (973-program) under Project No. 2013CB632501, the National Natural Science Foundation of China (NSFC) under the Nos. 11234012,

51222209, 51121064, and 50825205, the Shanghai Science and Technology Commission (Pujiang Program, 11PJ1410200). J.Y. thanks the NSFC (51028201) and NSFC-CAS/SAFEA International Partnership Program for Creative Research Teams, and International S&T Cooperation Program of China (2011DFB60150). J.R.S. and J.Y.C. acknowledge the support by GM and by the DOE under corporate agreement DE-FC26-04NT42278. X.S., J.Y., J.R.S., and J.Y.C. thank J. F. Herbst and M. W. Verbrugge for their continued support and encouragement. G.J.S. and S.W.C. thank the joint Caltech-Taiwan NSC program under the No. 101-3113-P-008-001.

Received: September 7, 2012
Revised: December 10, 2012
Published online: February 6, 2013

[1] C. Uher, in *Recent Trends in Thermoelectric Materials Research II*, Vol. *69* (Eds: T. M. Tritt), San Diego, USA **2000**, p. 139.
[2] T. M. Tritt, M. A. Subramanian, *MRS Bull.* **2006**, *31*, 188.
[3] B. C. Sales, D. G. Mandrus, B. C. Chakoumakos, in *Recent Trends in Thermoelectric Materials Research II*, Vol. *69* (Eds: T. M. Tritt), San Diego, USA **2000**, p. 1.
[4] G. A. Slack, in *CRC Handbook of Thermoelectrics*, Vol. *69* (Eds: D. M. Rowe), CRC, USA **1995**, p. 407.
[5] L. E. Bell, *Science* **2008**, *321*, 1457.
[6] G. S. Nolas, J. Poon, M. Kanatzidis, *MRS Bull.* **2006**, *31*, 199.
[7] E. S. Toberer, A. F. May, G. J. Snyder, *Chem. Mater.* **2010**, *22*, 624.
[8] X. Shi, W. Zhang, L. D. Chen, J. Yang, *Phys. Rev. Lett.* **2005**, *22*, 185 503.
[9] B. C. Sales, D. Mandrus, R. K. Williams, *Science* **1996**, *272*, 1325.
[10] H. Wagner, F. Dworschak, W. Schilling, *Phys. Rev. B* **1970**, *2*, 3856.
[11] D. C. Look, D. C. Reynolds, J. W. Hemsky, R. L. Jones, J. R. Sizelove, *Appl. Phys. Lett.* **1999**, *75*, 811.
[12] C. Frayret, A. Villesuzanne, M. Pouchard, *Chem. Mater.* **2005**, *17*, 6538.
[13] J. Callaway, H. C. Vonbaeyer, *Phys. Rev.* **1960**, *120*, 1149.
[14] A. K. Shukla, S. Ramdas, C. N. R. Rao, *J. Phys. Chem. Solids* **1973**, *34*, 761.
[15] R. Matejec, *Photographic Sci. Eng.* **1963**, *7*, 123.
[16] K. Kajihara, M. Hirano, L. Skuja, H. Hosono, in *Damage to VUV, EUV, and X-Ray Optics III*, Vol. *8077*. (Eds: L. Juha, S. Bajt, R. A. London), SPIE-Int. Soc. Opt. Eng., Bellingham **2011**.
[17] J. S. Dyck, W. D. Chen, C. Uher, L. Chen, X. F. Tang, T. Hirai, *J. Appl. Phys.* **2002**, *91*, 3698.
[18] X. Y. Li, L. D. Chen, J. F. Fan, W. B. Zhang, T. Kawahara, T. Hirai, *J. Appl. Phys.* **2005**, *98*, 083 702.
[19] M. Puyet, A. Dauscher, B. Lenoir, M. Dehmas, C. Stiewe, J. Hejtmanek, E. Muller, *J. Appl. Phys.* **2005**, *97*, 083 712.
[20] A. Leithe-Jasper, W. Schnelle, H. Rosner, M. Baenitz, A. Rabis, A. Gippius, E. N. Morozova, H. Borrmann, U. Burkhardt, R. Ramlau, U. Schwarz, J. A. Mydosh, Y. Grin, V. Ksenofontov, S. Reiman, *Phys. Rev. B* **2004**, *70*, 214 418.
[21] A. Rabis, A. Leithe-Jasper, A. A. Gippius, E. Morozova, M. Baenitz, W. Schnelle, N. Senthilkumaran, J. A. Mydosh, F. Steglich, Y. Grin, *J. Magn. Magn. Mater.* **2004**, *272*, 830.
[22] Y. Z. Pei, L. D. Chen, W. Zhang, X. Shi, S. Q. Bai, X. Y. Zhao, Z. G. Mei, X. Y. Li, *Appl. Phys. Lett.* **2006**, *89*, 451.
[23] Y. Z. Pei, L. D. Chen, W. Zhang, J. R. Salvador, J. H. Yang, *Appl. Phys. Lett.* **2009**, *95*, 042 101.
[24] L. D. Chen, T. Kawahara, X. F. Tang, T. Goto, T. Hirai, J. S. Dyck, W. Chen, C. Uher, *J. Appl. Phys.* **2001**, *90*, 1864.
[25] M. M. Koza, L. Capogna, A. Leithe-Jasper, H. Rosner, W. Schnelle, H. Mutka, M. R. Johnson, C. Ritter, Y. Grin, *Phys. Rev. B* **2010**, *81*, 174 302.
[26] B. K. Qin, X. L. Li, S. S. Li, T. C. Su, H. A. Ma, X. P. Jia, *J. Inorg. Mater.* **2010**, *25*, 23.
[27] G. S. Nolas, M. Kaeser, R. T. Littleton, T. M. Tritt, *Appl. Phys. Lett.* **2000**, *77*, 1855.
[28] X. Shi, H. Kong, C. P. Li, C. Uher, J. Yang, J. R. Salvador, H. Wang, L. Chen, W. Zhang, *Appl. Phys. Lett.* **2008**, *92*, 182 101.
[29] X. Shi, S. Q. Bai, L. L. Xi, J. Yang, W. Q. Zhang, L. D. Chen, J. H. Yang, *J. Mater. Res.* **2011**, *26*, 1745.
[30] X. Shi, J. Yang, J. R. Salvador, M. F. Chi, J. Y. Cho, H. Wang, S. Q. Bai, J. H. Yang, W. Q. Zhang, L. D. Chen, *J. Am. Chem. Soc.* **2011**, *133*, 7837.
[31] A. Harnwunggmoung, K. Kurosaki, T. Plirdpring, T. Sugahara, Y. Ohishi, H. Muta, S. Yamanaka, *J. Appl. Phys.* **2011**, *110*, 013 521.
[32] T. He, J. Z. Chen, H. D. Rosenfeld, M. A. Subramanian, *Chem. Mater.* **2006**, *18*, 759.
[33] R. C. Mallik, J. Y. Jung, S. C. Ur, I. H. Kim, *Metals Mater. Int.* **2008**, *14*, 223.
[34] R. C. Mallik, E. Mueller, I. H. Kim, *J. Appl. Phys.* **2012**, *111*, 023 708.
[35] B. C. Sales, B. C. Chakoumakos, D. Mandrus, *Phys. Rev. B* **2000**, *61*, 2475.
[36] R. P. Hermann, R. J. Jin, W. Schweika, F. Grandjean, D. Mandrus, B. C. Sales, G. J. Long, *Phys. Rev. Lett.* **2003**, *90*, 135 505.
[37] A. Leithe-Jasper, W. Schnelle, H. Rosner, R. Cardoso-Gil, M. Baenitz, J. A. Mydosh, Y. Grin, M. Reissner, W. Steiner, *Phys. Rev. B* **2008**, *77*, 064 412.
[38] A. Harnwunggmoung, K. Kurosaki, Y. Ohishi, H. Muta, S. Yamanaka, *J. Alloy. Compd.* **2011**, *509*, 1084.
[39] A. Sesselmann, T. Dasgupta, K. Kelm, E. Muller, S. Perlt, S. Zastrow, *J. Mater. Res.* **2011**, *26*, 1820.
[40] Y. Du, K. F. Cai, S. Chen, Z. Qin, S. Z. Shen, *J. Electron. Mater.* **2011**, *40*, 1215.
[41] J. K. Lee, S. M. Choi, W. S. Seo, H. L. Lee, I. H. Kim, *J. Korean Phys. Soc.* **2010**, *57*, 1010.
[42] W. Y. Zhao, C. L. Dong, P. Wei, W. Guan, L. S. Liu, P. C. Zhai, X. F. Tang, Q. J. Zhang, *J. Appl. Phys.* **2007**, *102*, 113 708.
[43] Z. Xiong, X. H. Chen, X. Y. Huang, S. Q. Bai, L. D. Chen, *Acta Mater.* **2010**, *58*, 3995.
[44] J. Y. Peng, J. He, Z. Su, P. N. Alboni, S. Zhu, T. M. Tritt, *J. Appl. Phys.* **2009**, *105*, 084 907.
[45] G. D. Tang, Z. H. Wang, X. N. Xu, Y. He, L. Qiu, Y. W. Du, *J. Electron Mater.* **2011**, *40*, 611.
[46] S. Ballikaya, G. Y. Wang, K. Sun, C. Uher, *J. Electron Mater.* **2011**, *40*, 570.
[47] H. Li, X. F. Tang, Q. J. Zhang, C. Uher, *Appl. Phys. Lett.* **2009**, *94*, 102 114.
[48] C. M. Jaworski, J. Tobola, E. M. Levin, K. Schmidt-Rohr, J. P. Heremans, *Phys. Rev. B* **2009**, *80*, 125 208.
[49] Y. Z. Pei, J. Lensch-Falk, E. S. Toberer, D. L. Medlin, G. J. Snyder, *Adv. Funct. Mater.* **2011**, *21*, 241.
[50] W. Y. Zhao, P. Wei, Q. J. Zhang, C. L. Dong, L. S. Liu, X. F. Tang, *J. Am. Chem. Soc.* **2009**, *131*, 3713.
[51] K. Ishida, M. Hasebe, N. Ohnishi, T. Nishizawa, *J. Less-Common Metals* **1985**, *114*, 361.
[52] T. Nishizawa, K. Ishida, *Metals Prog.* **1986**, *129*, 57.
[53] K. Ishida, T. Shumiya, H. Ohtani, T. Nishizawa, *J. Less-Common Metals* **1988**, *142*, 135.
[54] H. Enoki, K. Ishida, T. Nishizawa, *J. Less-Common Metals* **1990**, *160*, 153.
[55] K. M. Wunsch, E. Wachtel, *Z. Metallkunde* **1982**, *73*, 311.
[56] S. Q. Bai, Y. Z. Pei, L. D. Chen, W. Q. Zhang, X. Y. Zhao, J. Yang, *Acta Mater.* **2009**, *57*, 3135.
[57] G. Kresse, J. Hafner, *Phys. Rev. B* **1993**, *47*, 558.
[58] W. Dong, G. Kresse, J. Furthmuller, J. Hafner, *Phys. Rev. B* **1996**, *54*, 2157.
[59] L. Chaput, P. Pécheur, J. Tobola, H. Scherrer, *Phys. Rev. B* **2005**, *72*, 085 126.